applied sciences

MDPI

Article

Porous Materials Derived from Industrial By-Products for Titanium Dioxide Nanoparticles Capture

Antonella Cornelio, Alessandra Zanoletti, Stefania Federici, Laura Eleonora Depero and Elza Bontempi *

INSTM and Chemistry for Technologies Laboratory, Department of Mechanical and Industrial Engineering, University of Brescia, via Branze, 38, 25123 Brescia, Italy; a.cornelio001@unibs.it (A.C.); alessandra.zanoletti@unibs.it (A.Z.); stefania.federici@unibs.it (S.F.); laura.depero@unibs.it (L.E.D.)

* Correspondence: elza.bontempi@unibs.it

Received: 29 September 2020; Accepted: 13 November 2020; Published: 15 November 2020

check for updates

Abstract: The aim of this paper was the evaluation of hybrid porous materials, named SUNSPACE ("SUstaiNable materials Synthesized from by-Products and Alginates for Clean air and better Environment"), realized with raw materials such as silica fume (SUNSPACE SF) and bottom ash derived from municipal solid waste incineration (SUNSPACE BA), compared to cement and leaf for particulate matter (PM) entrapment. SUNSPACE BA was synthesized to overcome the limited applicability of the original material due to its dark grey color. The modification of raw materials used for its realization allows one to obtain a light color in comparison to the corresponding SUNSPACE SF, more suitable to be used as a coating on the buildings' facades for aesthetic reasons. Moreover, another great advantage was obtained by the synthesis of SUNSPACE BA in the frame of circular economy principles; indeed, it was obtained by using a waste material (derived from waste incineration), opening new possibilities for its reuse. Experimental tests to evaluate the particles entrapment capability of the material were realized for the first time by using a nanoparticles generator. TiO_2 suspension with a size of 300 nm and a concentration of 3 g/L was used to simulate a monodisperse nanoparticles flux. To compare the quantity of TiO_2 adsorbed by each specimen, both the exposed and the pristine samples were digested and then analyzed by total X-ray fluorescence (TXRF). The results showed a high adsorption capacity of SUNSPACE BA (3526 ± 30 mg/kg).

Keywords: airborne PM; nanoparticles; air quality; SUNSPACE; porous material; waste material; circular economy

1. Introduction

In the last few years, the control of air quality has become a very current topic. The impact of pollutants on the environment has been neglected for years. It is a cause of growing concern for the awareness of the risks to human health related to the characteristics of the air we breathe. According to [1], in Europe, 790,000 deaths per years are caused by environmental air pollution; one of the main culprits is particulate matter (PM).

PM is the most important pollutant in urban areas. It is composed of a complex mixture of solid and liquid particles of organic and inorganic substances suspended in the air [2].

In addition to being of natural origin, PM can also be produced from anthropogenic sources, such as domestic heating, industrial processes, and obviously traffic. Moreover, it can be directly emitted into the atmosphere, called primary aerosol, or can react with other substances present in the air, leading to the formation of secondary aerosol.

PM is characterized by long persistence times in the atmosphere and can therefore be transported even at a great distance from the emission point, considerably increasing the PM impact in a large part of the population.

Health risks due to PM are related to the particle size; PM_{10} (aerodynamic diameter ≤ 10 μm) can penetrate the upper part of the respiratory system up to the bronchi, while $PM_{2.5}$ (aerodynamic diameter ≤ 2.5 μm) can reach the lungs. Some studies reveal a correlation between the mortality for respiratory and cardiovascular diseases and the ultrafine PM [3–5]. The World Health Organization reveals that 30% of respiratory disease is caused by a high level of airborne PM [6]. Recent epidemiological episodes caused by COVID-19 have shown a high mortality rate in areas of Northern Italy that was attributed to the PM acting as a vector of the virus. However, very recent studies [7–9] have shown that, despite the fact that a direct correlation cannot be found, PM can be considered a dangerous pollution source. In particular, due to the high mortality rate recorded in the north of Italy, which is more polluted than the south, it cannot be excluded that the high rate of airborne pollution could be a co-factor. According to INEMAR (INventario EMissioni ARia) ARPA Lombardia (Agenzia Regionale per la Protezione dell'Ambiente) data, in Lombardy, one of the most polluted region of Italy, about 50% of primary PM_{10} emission is generated from non-industrial combustion (such as domestic heating), 20% from vehicles, 10% from industrial combustion, and the remaining part from other polluting sources [10].

People living in strongly polluted areas are subjected to very high levels of pollutants daily and are therefore more prone to suffer from respiratory and lung diseases favoring the attack by very aggressive viruses [11].

In addition, high concentrations of PM have negative effects not only on human health but also on economic and energy production levels. In recent years, in fact, the attention has focused on how airborne PM affects the production of energy through solar panels [12–14]. PM is responsible for 780 MW and 7400 MW of solar power reduction in India and China, respectively [15], with consequences also on the sector of investments in renewable energy.

It is evident that PM influences society in various ways, thus it is necessary to reduce PM concentrations in cities, especially to minimize citizens' exposure and health risks.

Filters are the conventional system widely adopted for PM entrapment. The materials used for their production are petroleum based (such as polystyrene or polypropylene). This makes the filter expensive and not competitive on the market. In addition, these materials have bad impacts on environment. As demonstrated in [16], the production of 1 kg of these polymers generates emissions in a range from 30 to 150 kg CO_{2eq} and requires high energy—more than 100 MJ.

Leaves currently represent the most sustainable low-cost materials for PM reduction. The airborne PM entrapment by vegetation is mainly driven by the interactions between particles and plant surfaces. It is influenced by particles size and by plants morphology such as roughness, hair, and wax cover [17]. Literature reports many works about the PM capture by plants. Generally, the species used are: Field maple such as *Acer campestre*, European ash such as *Fraxinus*, London plane such as *Platanus*, and Common Ivy such as *Hedera Helix* L., the widely used evergreen [18]. *Hedera Helix* L. has shown relatively high PM densities in all size fractions due to the important role of leaf surface wax in removing particles.

However, leaves alone are not able to capture such high quantities of PM and also have the disadvantage that most of them are not present during autumn and winter. Therefore, new approaches need to be found to address the problem. Given the great relevance of buildings in the urban context rather than green areas, the idea is to exploit these wide surfaces at our disposal by using porous materials to be applied on the buildings' facades. The advantage of these materials is not only the improvement of air quality but also the reuse of industrial by-products in the frame of circular economy principles.

The capability of porous material, named SUNSPACE ("SUstaiNable materials Synthesized from by-Products and Alginates for Clean air and better Environment") silica fume (SF), to trap fine and ultrafine particles has already been demonstrated in different studies [16,19–22]. SUNSPACE SF synthesis involves the use of industrial by-products such as silica fume, deriving from ferro-silicon processing. The idea is to apply SUNSPACE SF as plaster on urban surfaces. Unfortunately, its dark color surely represents an aesthetic limit for the application as a plaster. In order to overcome this limit and to use sustainable materials to depollute urban air [16], a variation to the SUNSPACE SF formulation is here proposed. For this aim, the idea was to use a different raw material but with the aim to improve the sustainability of the construction sector. In particular, the use of secondary materials in building application is still limited. This work shows for the first time the use of bottom ash for the synthesis of a lighter colored porous material. This waste is the main residue produced from the incineration of municipal solid waste. It is estimated that 16 Mt of bottom ash are produced each year in Europe (EUROSTAT), posing a significant waste management challenge. The chemical composition of bottom ash is very similar to that of some cementitious and ceramic materials, providing a source of sustainable supply of secondary raw materials for a greener and more circular economy [23]. In this work, bottom ash was used instead of silica fume. The aim of this paper was to compare these hybrid porous materials (SUNSPACE SF and SUNSPACE bottom ash (BA)) with cement and *Hedera Helix* L. leaf. The last one was used as a reference due to its ability in airborne PM entrapment, as confirmed in different studies [24]. As discussed in literature, the small size and the large surface area of nanoparticles may cause adverse effects on environment and human health, particularly neurologically. As reported in literature, titanium dioxide nanoparticles are widely used in different applications such as paints, coating, building materials, wastewater treatment, additives in pharmaceutical, food colorants, and cosmetics [25–27]. Due to the complexity in the chemistry and the different available dimensions of real PM sources [22], a model experiment was settled. In particular, titanium dioxide was selected to simulate the aerosol PM dispersion, and a generator was used to generate the PM flux. Then, this work was devoted to study nanoparticles entrapment. The work was performed in the frame of Azure chemistry approach; indeed, it demonstrates that it is possible to use a waste material to remediate the environment [16].

2. Materials and Methods

2.1. Materials and Reagents

Calcium iodate ($Ca(IO_3)_2$, CAS number: 7789-80-2) and sodium alginate (SA, CAS number: 9005-38-3) were provided by Sigma Aldrich. Sodium bicarbonate ($NaHCO_3$, CAS number: 14455-8, ≥99.8% w/w) was bought in a local store. Silica fume was kindly supplied by Metalleghe spa, Brescia, Italy. Calcium hydroxide ($Ca(OH)_2$, CAS number: 1305-62-0) and bottom ash were provided by Brescia municipal solid waste incinerator plant managed by A2A spa. Cement (TECNOCEM- 42.5 class) was provided by Italcementi, Bergamo. *Hedera Helix* L. leaves were collected before carrying out the experiments in a town near Brescia. MilliQ water (Millipore DirectQ-5 purification system) was used for the synthesis of the samples and for the titanium dioxide (TiO_2) suspension preparation. Titanium dioxide powder (Hombitan 97% with 300 nm size) was selected as PM nanoparticles. It was kindly supplied by Rifra Masterbatches spa.

2.2. Samples Synthesis

SUNSPACE SF samples were prepared as already described in [21]. Briefly, 25 mL of milliQ water were mixed with 0.6 g of sodium alginate and 1 g of calcium iodate (as binder) until the gel solution was formed. Finally, 17.88 g of silica fume and 5 g of sodium bicarbonate (as pore former) were added to the compound. After manually separating the fraction greater than 2 cm, the bottom ash was dried at 100 °C for 1 h. Then, bottom ash was sieved to obtain a fraction lower than 300 µm. SUNSPACE BA samples were made by mixing 32 mL of milliQ water with 0.6 g of sodium alginate and 1 g of calcium iodate. Then, 9 g of bottom ash and 9 g of calcium hydroxide were added, and finally 5 g of sodium bicarbonate were mixed with the compound. Cement was crumbled into a MM400 ball vibratory mill for 3 min at a frequency of 25 Hz with one sphere of 20 mm diameter, obtaining a powder with particle size in a range from 106 to 300 µm. A total of 17 g of cement were mixed with 6.8 mL of milliQ water (water:cement ratio 0.4). The slurries obtained from three samples were inserted in circular aluminum molds (2.73 ± 0.21) cm of diameter and put on heating plates for 1 h at low temperature (70–80 °C). In order to have the same exposed surface (5.9 ± 0.5) cm^2 for all the samples, the leaves of *Hedera Helix* L. were cut to obtain 4 samples of 2.7 cm in diameter. Before exposure, leaves samples were carefully washed with milliQ water to eliminate any impurities present.

2.3. Characterization Techniques

Colorimetric analysis was performed by UV-Vis Spectroscopy-Color Measurement Minolta CM 2600d.

Structural characterization was performed on the three materials by X-ray diffraction (XRD) by mean with Panalytical diffractometer (Netherlands), using Cu Ka (1.5406 Å) radiation and operating at 40 kV and 40 mA. Morphological analysis of the samples was performed by stereomicroscopy (Leica MZ 16 A coupled with software Leica Qwin) and by a LEO EVO 40 scanning electron microscopy (SEM) (Zeiss).

2.4. Nanoparticles Generator Tests

The capability of air particulate matter entrapment of different materials was investigated for the first time through laboratory tests by using a nanoparticles generator (Grimm aerosol, Particle-Generator MODEL 7.811). The dispersion of nanoparticles in the air was simulated with the generator using the titanium dioxide suspension as monodisperse PM source.

The TiO_2 suspension (using a monodisperse TiO_2 powder with the size of 300 nm) was prepared by mixing 0.45 g of powder with 150 mL of milliQ water to obtain a final concentration of about 3 g/L. Then, the suspension was sonicated for 15 min.

After several tests carried out to optimize the experimental set up, the following operating parameters were settled: atomizer pressure about 290 mbar, flow of the dryer 7 L/min, and volume of titanium dioxide suspension between 5 and 7 mL. The choice of this volume was made for the generator specification requirement to avoid the reduction of particles production rate and the shift of particles size distribution. The tests were carried out having both PM generator and samples inside the glove box to avoid the emission of TiO_2 nanoparticles flow into the atmosphere. The samples were positioned on a fixed support in front of the generator outlet at the same height (15 cm) and 2 cm away from it. The experimental set-up is reported in Scheme 1.

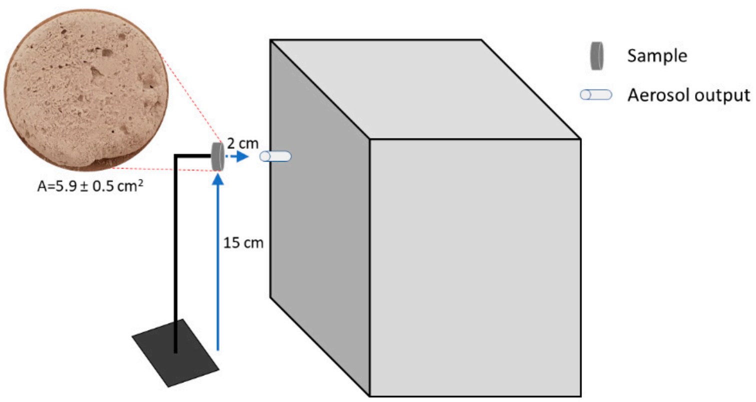

Scheme 1. Experimental set up: "SUstaiNable materials Synthesized from by-Products and Alginates for Clean air and better Environment" (SUNSPACE) bottom ash (BA) sample placed at 15 cm of height and 2 cm distance from the particulate matter (PM) generator outlet.

The tests were conducted by exposing the samples to aerosol titanium dioxide nanoparticles flow for 4 min after 1 min of PM generator stabilization. A total of 3 specimens were tested for each material as independent replicates. Unlike other materials, the TiO_2 suspension remained in aqueous form on the leaf surface.

2.5. Preparation of Samples for Digestion

To compare the quantity of titanium dioxide adsorbed by each specimen, both the exposed and the pristine samples were digested. After the PM exposure, all samples were carefully shaken 3 times to eliminate any titanium dioxide excess and were eventually aggregated onto the samples surface. Then, SUNSPACE SF, SUNSPACE BA, and cement were superficially scratched to remove the regions where titanium dioxide nanoparticles were accumulated. About 0.25 g of powders were obtained for porous samples, while the leaf samples (about 0.085 g) were completely digested. According to the EPA method 3052 for siliceous matrices [20], the sample powders and the leaves were put in a Teflon vessel with 4 mL of HNO_3 (≥65%), 2 mL of HCl (37%), and 2 mL of HF (48%). Each vessel was processed by the CEM SP-D 10/35 microwave digestion system (CEM Corporation, Matthews, United States) through five steps: 160 °C for 3 min, 180 °C for 5 min, 200 °C for 3 min, 205 °C for 5 min, and 210 °C for 10 min. Finally, the volume of each sample was adjusted to 50 mL with milliQ water.

2.6. Total X-ray Fluorescence Analysis of Solutions

The evaluation of the titanium concentration was performed by total reflection X-ray fluorescence (TXRF) spectrophotometer equipped with Mo anode (S2 PICOFOX, Bruker AXS Microanalysis GmbH, Berlin, Germany) operating at 750 μA and 50 kV. For the quantification, Ga, as internal standard, was added to the digested samples in a concentration equal to 1 mg/L. Ga stock solution (1000 mg/L) was provided by Sigma Aldrich. A drop of 10 μL of the solution was deposited in the center of a plexiglass circular support and dried on a heating plate at 50 °C. Plexiglass reflectors were used due to the presence of HF. Three specimens for each sample were prepared. Spectra Plus 5.3 (Bruker AXS Microanalysis GmbH, Berlin, Germany) was used for the spectra evaluation.

3. Results and Discussion

3.1. Characterization of Samples

The use of bottom ash instead of silica fume allowed the realization of lighter porous sample, as shown in Figure 1. The colorimetric analysis defines a color space through CIELAB coordinates: L (luminance) and two-color channels (a and b). L ranged from 0 (dark) to 100 (white), while a and b changed from negative to positive values (green < a < red and blue < b < yellow). SUNSPACE changed its color from dark grey (L = 39.83) to light grey (L = 81.97) using bottom ash instead of silica fume, as reported in Table 1. The improvement of the color represents an advantage for the development of the material as plaster on urban buildings.

SUNSPACE SF spectrum, as already reported in [21], was characterized by a large halo between 15–30° (2Θ) due to the presence of amorphous phase, such as silica fume. Cristobalite (SiO_2) and sodium iodate hydrate ($NaIO_3 \cdot H_2O$) peaks were identified in the spectrum. This last phase was formed during the material synthesis. On the contrary, SUNSPACE BA was characterized by calcite ($CaCO_3$), quartz (SiO_2), and ettringite ($Ca_6Al_2(SO_4)_3(OH)_{12} \cdot 26H_2O$) due to the presence of bottom ash and calcium hydroxide used in the material synthesis [28]. In addition, as in the SUNSPACE SF spectrum, some sodium iodate hydrate peaks were identified, generated during the material synthesis. Finally, the main crystalline phases of the cement sample were calcite ($CaCO_3$) and calcium silicate oxide ($Ca_3(SiO_4)O$). Some peaks could be attributed to ettringite ($Ca_6Al_2(SO_4)_3(OH)_{12} \cdot 26H_2O$), gypsum ($CaSO_4 \cdot 2H_2O$), grossular $Ca_3Al_2(SiO_4)_3$, and iron oxide calcium oxide ($Fe_2O_3(CaO)_2$).

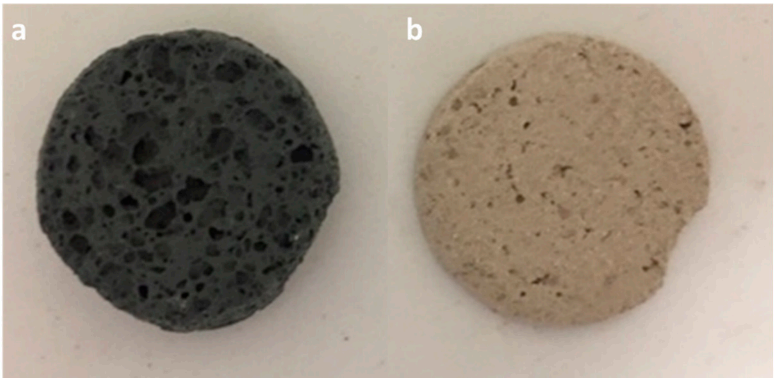

Figure 1. Optical images of SUNSPACE SF (**a**) and SUNSPACE BA (**b**).

Table 1. Results of colorimetric analysis made on SUNSPACE SF and SUNSPACE BA. Data were evaluated including SCI and excluding SCE specular component.

	SUNSPACE SF		SUNSPACE BA	
	SCI	**SCE**	**SCI**	**SCE**
L	39.83	39.61	81.97	81.49
a	−0.92	−0.87	0.77	0.80
b	−2.33	−2.36	6.34	6.22

Figure 2 shows the XRD spectra of SUNSPACE SF, SUNSPACE BA, and cement samples.

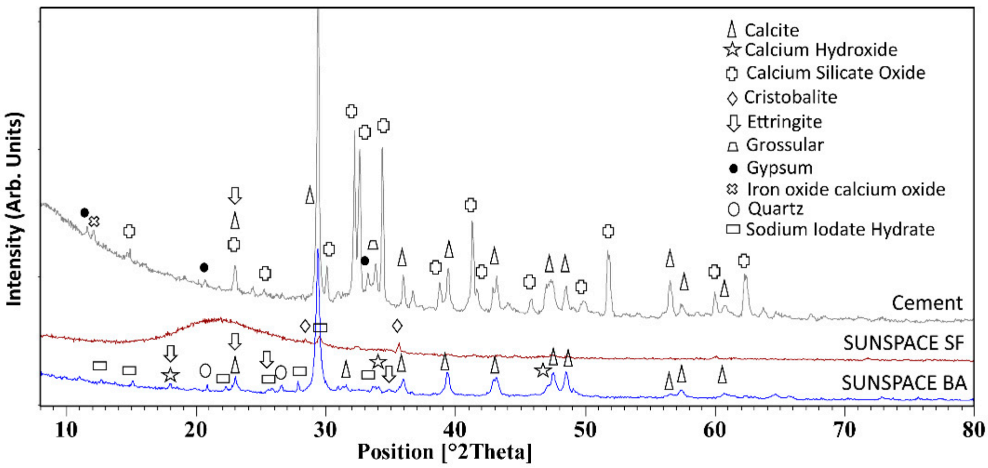

Figure 2. X-ray diffraction (XRD) patterns of SUNSPACE SF, SUNSPACE BA and cement samples.

Figure 3 shows the optical microscopy images collected on all samples. The presence of macro pores on SUNSPACE SF (Figure 3a) and SUNSPACE BA (Figure 3b) was evident, while cement material (Figure 3c) showed a uniform surface with smaller pores in dimensions. The image of *Hedera Helix* L. (Figure 3d) surface showed no evident pores, very likely due to the low magnification of the image, but the presence of voids between the long tubules that promote fine PM capture was already reported in a previous work [20].

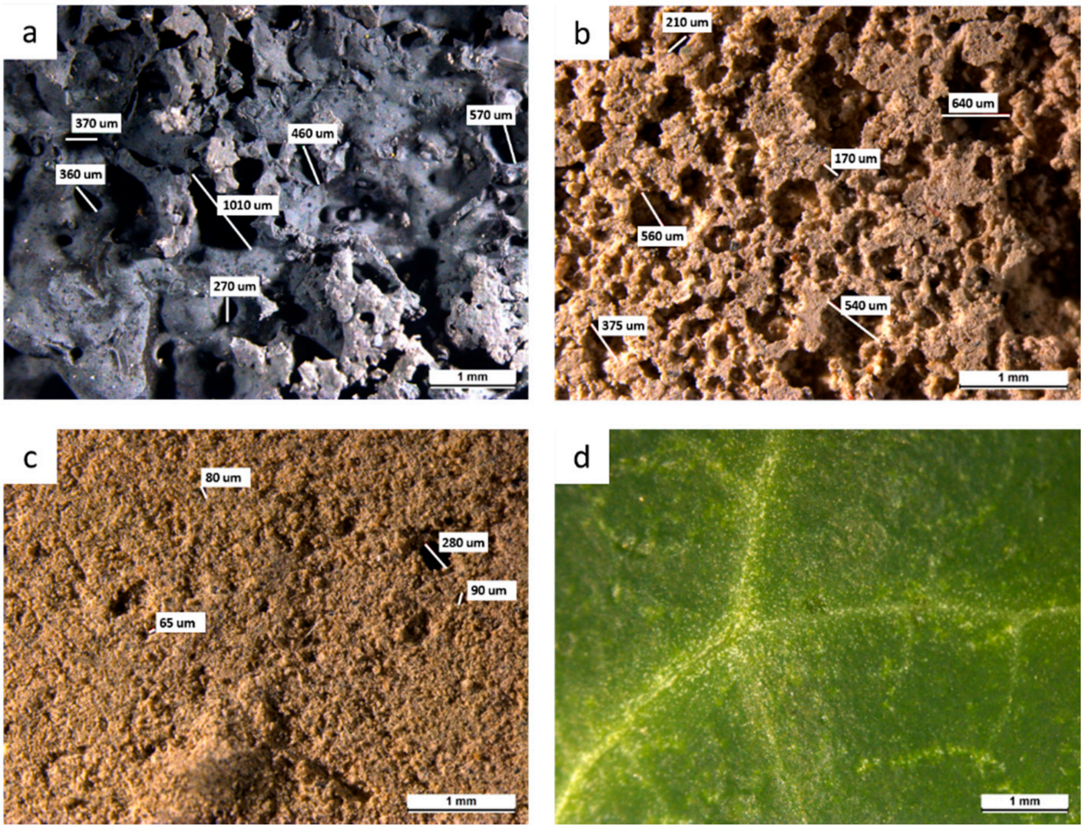

Figure 3. Optical microscopy images of SUNSPACE SF (**a**), SUNSPACE BA (**b**), cement material (**c**) and *Hedera Helix* L. leaf (**d**).

Figure 4 shows SEM images of SUNSPACE BA at different magnifications (a and b), SUNSPACE SF (c), and cement material (d). As reported in Assi et al. [28], bottom ash with particle size lower than 300 µm was mainly characterized by amorphous phase (60%), suggesting its high reactivity with calcium hydroxide. Indeed, SUNSPACE BA, unlike the other two samples, showed a fibrillar matrix, clearly visible in the Figure 4b, due to the C-S-H formation typical of pozzolanic reaction [29]. This branched morphology may have a positive influence on PM adsorption, promoting particles entrapment in the sample. According to [21], SUNSPACE SF is characterized by spherical particles of silica, with size dimensions from 20 to 700 nm, agglomerated together. Macro pores with dimensions of some µm were clearly identified on the SUNSPACE SF surface, as reported in Figure 4c. In a recent paper, it was shown that SUNSPACE SF contains not only macro pores but also ink bottle shaped pores in order to nm. The cement sample showed irregular needle-like structures, probably attributed to cement hydration products as ettringite. As reported in literature, its formation is caused by the reaction between calcium sulfate and calcium aluminate, available in a cementitious matrix [30,31]. The formation of ettringite prevents flash setting and improves mechanical strength [30].

Morphological characterization of *Hedera Helix* L. was already published in a previous work [20]. SEM analysis revealed that the leaf surface has epicuticular wax in the shape of long tubules with size less than 2 µm. The voids between these tubules promotes fine PM capture. As reported and discussed in literature, *Hedera Helix* L. shows high PM densities accumulation in all size fractions due to the presence of surface wax [24,32].

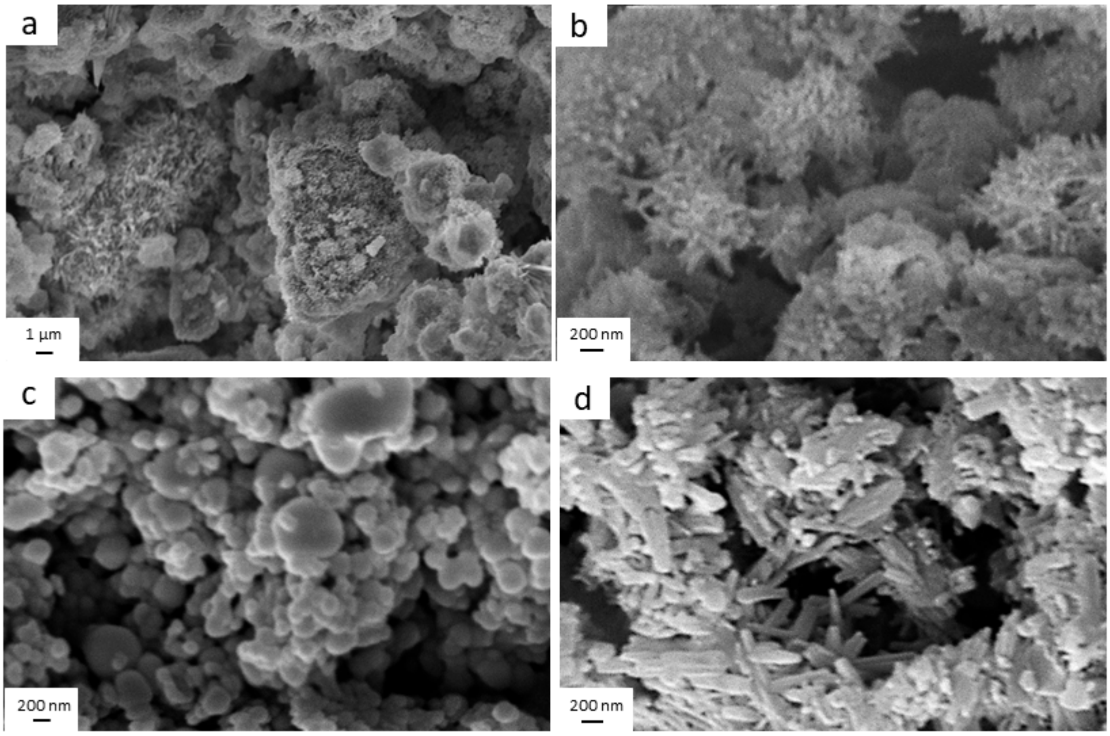

Figure 4. SEM images of SUNSPACE BA at different magnifications (**a**,**b**), SUNSPACE SF (**c**), and cement material (**d**).

3.2. TiO_2 Nanoparticles Adsorption Capability

The analysis of the concentration of aerosol titanium dioxide nanoparticles adsorbed by samples was necessary to evaluate the adsorption capacity of each material. This evaluation was performed comparing pristine and exposed materials. Figure 5 reports the results of the titanium dioxide concentrations (expressed in mg/kg) presented on samples before (pristine material) and after (exposed material) the exposure to TiO_2 in logarithmic scale.

SUNSPACE BA had the best adsorption capacity, probably due to its branched morphology that may favor the PM entrapment.

Even the leaf showed high concentrations of titanium dioxide deposited onto its surface; these values were probably due to the fact that the titanium dioxide suspension was deposited on the leaf surface without actually being adsorbed. SUNSPACE SF seemed to show lower adsorption capacity than SUNSPACE BA. As reported in [21], this material was characterized not only by macro pores but also ink bottle shaped pores in order to nm. Especially, the hysteresis loops observed in the N_2 physisorption isotherms revealed pores with narrowing sizes of about 15–30 nm and swelling more than 150 nm [21]. This shape probably hindered the penetration of titanium dioxide nanoparticles, with sizes of about 300 nm, in the pores. In fact, the ability of SUNSPACE SF to trap titanium dioxide nanoparticles with lower dimensions (about 25 nm) was demonstrated in a previous paper [20]. Cement had no adsorption capacity because it was clearly characterized by few pores, as shown in Figure 3c.

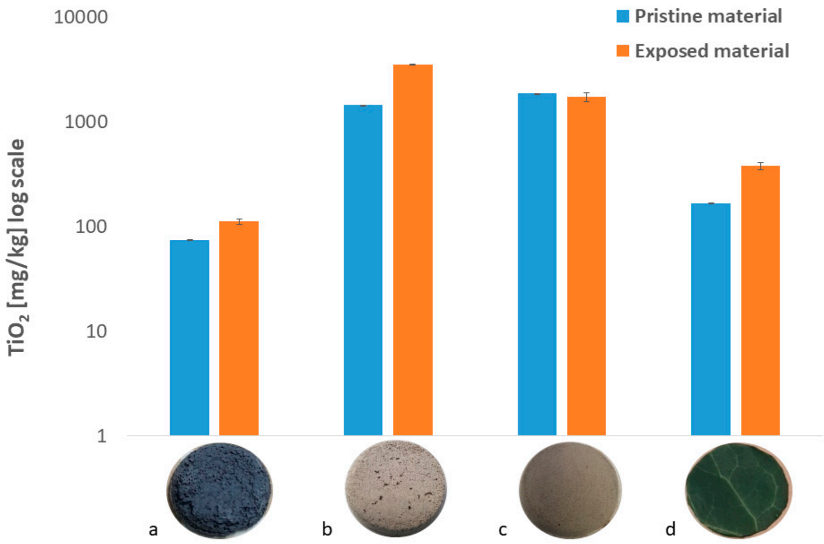

Figure 5. Titanium dioxide adsorption on samples expressed in logarithmic scale: SUNSPACE SF (**a**), SUNSPACE BA (**b**), cement material (**c**), and *Hedera Helix* L. (**d**).

4. Conclusions

This work aimed to propose a modification of SUNSPACE material and evaluate its adsorption capability by using a model experiment with titanium dioxide nanoparticles. For this purpose, two porous materials derived from industrial by-products were compared. SUNSPACE SF was synthesized by using silica fume as raw material, while SUNSPACE BA was produced by using coarse residues of municipal solid incinerator plant. The ability of these materials in particulate matter trap was compared to cement and *Hedera Helix* L., the leaf widely used in PM adsorption. TiO_2 with the size of 300 nm was used to simulate PM dispersion.

SUNSPACE BA revealed the best performance in comparison to the other porous sample. In addition, the lighter color of this material in comparison with SUNSPACE SF had the greatest aesthetic prerequisites, making this material suitable to be applied as plaster in an urban area.

Author Contributions: Conceptualization, E.B.; formal analysis, A.C., A.Z.; investigation, A.C., A.Z., S.F.; data curation, S.F.; writing—original draft preparation, A.C., A.Z., and E.B.; writing—review and editing, E.B., L.E.D.; supervision, E.B.; project administration, E.B. and L.E.D.; funding acquisition, E.B. and L.E.D. All authors have read ad agreed to the published version of the manuscript.

Funding: This research in the frame of the project: "Energy recovery of waste sludge and their re-use as an alternative to some natural resources, for the production of Green composites, RENDERING" is funded by Ministero dell'Ambiente e della Tutela del Territorio e del Mare-Direzione generale per i rifiuti e l'inquinamento. It is supported by University of Brescia, CSMT, INSTM, and Regione Lombardia.

Acknowledgments: Authors thank Leonardo Lauri for SEM analysis.

Conflicts of Interest: The authors declare no conflict of interest.

References

1. Lelieveld, J.; Klingmu, K.; Pozzer, A.; Po, U.; Fnais, M.; Daiber, A.; Mu, T. Cardiovascular disease burden from ambient air pollution in Europe reassessed using novel hazard ratio functions. *Eur. Heart J.* **2019**, *40*, 1590–1596. [CrossRef] [PubMed]
2. WHO Ambient (Outdoor) Air Pollution. Available online: https://www.who.int/news-room/fact-sheets/detail/ambient-(outdoor)-air-quality-and-health (accessed on 29 September 2020).
3. Hoffmann, B.; Moebus, S.; Dragano, N.; Stang, A.; Möhlenkamp, S.; Schmermund, A.; Memmesheimer, M.; Bröcker-Preuss, M.; Mann, K.; Erbel, R.; et al. Chronic residential exposure to particulate matter air pollution and systemic inflammatory markers. *Environ. Health Perspect.* **2009**, *117*, 1302–1308. [CrossRef] [PubMed]

4. Nemmar, A.; Hoylaerts, M.F.; Hoet, P.H.M.; Vermylen, J.; Nemery, B. Size effect of intratracheally instilled particles on pulmonary inflammation and vascular thrombosis. *Toxicol. Appl. Pharmacol.* **2003**, *186*, 38–45. [CrossRef]
5. Xing, Y.F.; Xu, Y.H.; Shi, M.H.; Lian, Y.X. The impact of PM2.5 on the human respiratory system. *J. Thorac. Dis.* **2016**, *8*, E69–E74. [PubMed]
6. WHO. More testing for HIV needed WHO's global air-quality guidelines. *Lancet* **2006**, *2006*, 1–496.
7. Bontempi, E. First data analysis about possible COVID-19 virus airborne diffusion due to air particulate matter (PM): The case of Lombardy (Italy). *Environ. Res.* **2020**, *186*, 109639. [CrossRef] [PubMed]
8. Kissler, S.M.; Tedijanto, C.; Goldstein, E.; Grad, Y.H.; Lipsitch, M. Projecting the transmission dynamics of SARS-CoV-2 through the postpandemic period. *Science* **2020**, *368*, 860–868. [CrossRef]
9. Bontempi, E.; Vergalli, S.; Squazzoni, F. Understanding COVID-19 diffusion requires an interdisciplinary, multi-dimensional approach. *Environ. Res.* **2020**, *188*, 109814. [CrossRef]
10. ARPA INEMAR, INventario EMissioni Aria. Available online: https://www.inemar.eu/xwiki/bin/view/Inemar/WebHome (accessed on 24 September 2020).
11. Conticini, E.; Frediani, B.; Caro, D. Can atmospheric pollution be considered a co-factor in extremely high level of SARS-CoV-2 lethality in Northern Italy? *Environ. Pollut.* **2020**, *261*, 114465. [CrossRef]
12. Zhou, L.; Schwede, D.B.; Wyat Appel, K.; Mangiante, M.J.; Wong, D.C.; Napelenok, S.L.; Whung, P.Y.; Zhang, B. The impact of air pollutant deposition on solar energy system efficiency: An approach to estimate PV soiling effects with the Community Multiscale Air Quality (CMAQ) model. *Sci. Total Environ.* **2019**, *651*, 456–465. [CrossRef]
13. Peters, I.M.; Karthik, S.; Liu, H.; Buonassisi, T.; Nobre, A. Urban haze and photovoltaics. *Energy Environ. Sci.* **2018**, *11*, 3043–3054. [CrossRef]
14. Fattoruso, G.; Nocerino, M.; Sorrentino, G.; Manna, V.; Fabbricino, M.; Di Francia, G. *Estimating Air Pollution Related Solar Insolation Reduction in the Assessment of the Commercial and Industrial Rooftop Solar PV Potential*; Springer: Cham, Switzerland, 2020; pp. 1–13.
15. Bergin, M.H.; Ghoroi, C.; Dixit, D.; Schauer, J.J.; Shindell, D.T. Large reductions in solar energy production due to dust and particulate air pollution. *Environ. Sci. Technol. Lett.* **2017**, *4*, 339–344. [CrossRef]
16. Zanoletti, A.; Bilo, F.; Depero, L.E.; Zappa, D.; Bontempi, E. The first sustainable material designed for air particulate matter capture: An introduction to Azure Chemistry. *J. Environ. Manag.* **2018**, *218*, 355–362. [CrossRef] [PubMed]
17. Petroff, A.; Mailliat, A.; Amielh, M.; Anselmet, F. Aerosol dry deposition on vegetative canopies. Part I: Review of present knowledge. *Atmos. Environ.* **2008**, *42*, 3625–3653. [CrossRef]
18. Dzierzanowski, K.; Popek, R.; Gawrońska, H.; Saebø, A.; Gawroński, S.W. Deposition of particulate matter of different size fractions on leaf surfaces and in waxes of urban forest species. *Int. J. Phytoremediation* **2011**, *13*, 1037–1046. [CrossRef]
19. Zanoletti, A.; Bilo, F.; Federici, S.; Borgese, L.; Depero, L.E.; Ponti, J.; Valsesia, A.; La Spina, R.; Segata, M.; Montini, T.; et al. The first material made for air pollution control able to sequestrate fine and ultrafine air particulate matter. *Sustain. Cities Soc.* **2020**, *53*, 101961. [CrossRef]
20. Zanoletti, A.; Bilo, F.; Borgese, L.; Depero, L.E.; Fahimi, A.; Ponti, J.; Valsesia, A.; La Spina, R.; Montini, T.; Bontempi, E. SUNSPACE, a porous material to reduce air particulate matter (PM). *Front. Chem.* **2018**, *6*, 534. [CrossRef]
21. Zanoletti, A.; Vassura, I.; Venturini, E.; Monai, M.; Montini, T.; Federici, S.; Zacco, A.; Treccani, L.; Bontempi, E. A new porous hybrid material derived from silica fume and alginate for sustainable pollutants reduction. *Front. Chem.* **2018**, *6*, 60. [CrossRef]
22. Bilo, F.; Zanoletti, A.; Borgese, L.; Depero, L.E.; Bontempi, E. Chemical analysis of air particulate matter trapped by a porous material, synthesized from silica fume and sodium alginate. *J. Nanomater.* **2019**, *2019*, 1–9. [CrossRef]
23. Lederer, J.; Michal, Š.; Franz-Georg, S.; Margarida, Q.; Jiri, H.; Florian, H.; Valerio, F.; Johann, F.; Roberto, B.; Elza, B.; et al. What waste management can learn from the traditional mining sector: Towards an integrated assessment and reporting of anthropogenic resources. *Waste Manag.* **2020**, *113*, 154–156.
24. Weerakkody, U.; Dover, J.W.; Mitchell, P.; Reiling, K. Particulate matter pollution capture by leaves of seventeen living wall species with special reference to rail-traffic at a metropolitan station. *Urban For. Urban Green.* **2017**, *27*, 173–186. [CrossRef]

25. Meena, R.; Kumar, S.; Paulraj, R. Titanium oxide (TiO_2) nanoparticles in induction of apoptosis and inflammatory response in brain. *J. Nanoparticle Res.* **2015**, 17. [CrossRef]
26. Wilczyńska-Michalik, W.; Rzeźnikiewicz, K.; Pietras, B.; Michalik, M. Fine and ultrafine TiO_2 particles in aerosol in Kraków (Poland). *Mineralogia* **2014**, *45*, 65–77. [CrossRef]
27. Wang, J.; Liu, Y.; Jiao, F.; Lao, F.; Li, W.; Gu, Y.; Li, Y.; Ge, C.; Zhou, G.; Li, B.; et al. Time-dependent translocation and potential impairment on central nervous system by intranasally instilled TiO_2 nanoparticles. *Toxicology* **2008**, *254*, 82–90. [CrossRef]
28. Assi, A.; Bilo, F.; Federici, S.; Zacco, A.; Depero, L.E.; Bontempi, E. Bottom ash derived from municipal solid waste and sewage sludge co-incineration: First results about characterization and reuse. *Waste Manag.* **2020**, *116*, 147–156. [CrossRef]
29. Assi, A.; Bilo, F.; Zanoletti, A.; Ponti, J.; Valsesia, A.; La Spina, R.; Zacco, A.; Bontempi, E. Zero-waste approach in municipal solid waste incineration: Reuse of bottom ash to stabilize fly ash. *J. Clean. Prod.* **2020**, *245*, 118779. [CrossRef]
30. Barger, G.S.; Bayles, J.; Blair, B.; Brown, D.; Chen, H.; Conway, T.; Hawkins, P. *Ettringite Formation and the Performance of Concrete*; Portland Cement Association: Skokie, IL, USA, 2001; pp. 1–16.
31. Chrysochoou, M.; Dermatas, D. Evaluation of ettringite and hydrocalumite formation for heavy metal immobilization: Literature review and experimental study. *J. Hazard. Mater.* **2006**, *136*, 20–33. [CrossRef]
32. Chen, L.; Liu, C.; Zhang, L.; Zou, R.; Zhang, Z. Variation in Tree Species Ability to Capture and Retain Airborne Fine Particulate Matter (PM2.5). *Sci. Rep.* **2017**, *7*, 1–11. [CrossRef]